Exploring the inner region of NGC 1316 through CO ALMA data

J. Saponara[1], M.V. Reynaldi[2,3], A.V. Smith Castelli[2,3], F.R. Faifer[2,3], P. Benaglia[1], L.A. Sesto[2,3] & C.G. Escudero[2,3]

[1] *Instituto Argentino de Radioastronomía, CONICET–CICPBA–UNLP, Argentina*
[2] *Facultad de Ciencias Astronómicas y Geofísicas, UNLP, Argentina*
[3] *Instituto de Astrofísica de La Plata, CONICET–UNLP, Argentina*

Contact / jsaponara@iar.unlp.edu.ar

Resumen / La galaxia NGC 1316 (Fornax A) es el remanente de una fusión, y es el objecto más brillante del cúmulo de Fornax. Además, es la tercer radiogalaxia más cercana a la Vía Lactea ($D = 20.8 \pm 0.5$ Mpc) y alberga un núcleo activo. Debido a la complejidad de ésta fuente, en una variedad de escalas y componentes, la misma fue observada en diferentes longitudes de onda. Imágenes ópticas profundas revelaron estructuras complejas, en sus regiones externas, como arcos y bucles, mientras que las observaciones en el infrarrojo lejano muestran presencia de polvo en su parte interna, el cual es responsable de una fuerte extinción. A su vez, el polvo se encuentra distribuido conformando distintas estructuras que incluyen un arco al noroeste, un grumo al sureste, una componente extendida hacia el suroeste y nubes de polvo entre ellos. Algunas de estas características también están bien delineadas por la presencia del CO. En trabajos anteriores, a partir de datos en continuo de radio, se informó que en la región nuclear el jet presenta una estructura de "S", lo cual sugiere una interacción entre el *jet* y el medio interestelar de la galaxia. NGC 1316 es un objeto notable porque alberga una subpoblación importante de cúmulos globulares jóvenes. Para comprender mejor la historia y los procesos físicos que están teniendo lugar actualmente en la región interior de NGC 1316, comenzamos a recopilar datos públicos en varios rangos espectrales, de instrumetos como ALMA, VLA, Chandra y HST. En este trabajo nos centramos en los datos disponibles de CO(J=2-1) de ALMA y la información que se puede recuperar de ellos.

Abstract / The merger remnant NGC 1316 (Fornax A) is the brightest galaxy in the Fornax cluster, and it is the third nearest radio-bright galaxy ($D = 20.8 \pm 0.5$ Mpc) hosting an Active Galactic Nuclei. Due to the complexity of this source, on a variety of scales and components, it was observed at different wavelengths. Deep optical images revealed complex structures such as ripples and loops in its outer regions, while far-infrared observations show prominent dust extinction in its inner part. The dust is found in diverse structures that include a north-west shell, a south-east blob, an extended component to the south-west, and dust patches among them. Some of these features are well traced by CO as well. The presence of a bent nuclear jet was reported in previous works, after radio continuum observations, suggesting an interaction between the jet and the interstellar medium of the galaxy. NGC 1316 is a remarkable object because it harbours a notable subpopulation of young globular clusters. To better understand the history and the physical processes that are currently taking place in the inner region of NGC 1316, we started to gather the public data at various spectral ranges, from instruments such as ALMA, VLA, Chandra and HST. In this poster, we will focus on the available CO(J=2-1) ALMA data, and the information that could be retrieved from them.

Keywords / galaxies: individual (NGC 1316) — Galaxy: structure

1. Introduction

NGC 1316 (Fornax A) is the brightest galaxy of the Fornax cluster, member of an infalling subgroup from the outskirts of the cluster ($D = 20.8 \pm 0.5$ Mpc, Cantiello et al., 2013). It is the third nearest radio-bright galaxy (Maccagni et al., 2020), and it hosts an Active Galactic Nuclei (AGN) with extended radio lobes (33 arcmin, Mackie & Fabbiano, 1998). The presence of a bent nuclear jet was reported by different authors (e.g. Ekers et al., 1983), suggesting the interaction between the jet and the interstellar medium of the galaxy. Recently, Maccagni et al. (2020) proposed that the AGN of NGC 1316 is rapidly flickering from an active nuclear phase to a non-active one. In this scenario, the central emission detected at radio frequencies would not be the remnant of the active phases that formed the lobes but it would be tracing the recent activity of the AGN.

NGC 1316 is a merger remnant as indicated by deep optical images that revealed complex structures such as ripples and loops in the outer regions (Schweizer, 1980, 1981; Iodice et al., 2017), while mid-infrared observations show prominent amount of dust in the inner part of the galaxy (Duah Asabere et al., 2016). The dust displays a complex structure that includes a shell in the NW, a blob in the SE, an extended structure to the SW, and several dust clouds between them (Duah Asabere et al., 2016). Some of these features are well traced by CO observations (Morokuma-Matsui et al., 2019), showing that molecular gas is mixed within dust. The merger remnant scenario is also supported by the identification of young globular clusters (GCs), as reported by Sesto et al. (2016).

In order to better understand the history and the physical processes that are currently taking place in NGC 1316, we started to work with archival Atacama Large Millimiter Array (ALMA) data. In Section 2, we describe the ALMA data, in Section 3 we present our results, followed by the future work in Section 4.

2. ALMA data

We used the Band 6 ($\approx$ 230 GHz) ALMA public data of the program ID = #2017.1.01140.S, obtained during May 2018. The observations were performed with the 7m antennae (7M) array and the total integration time on the source was $\approx$ 53 min. It covered CO(J=2-1) emission at the rest-frame frequency of $\nu_{\rm rest} \approx 230.538$ GHz. The angular resolution achieved is $5.48'' \times 4.30''$. The r.m.s. in the final image cube is 0.7 Jy beam^{-1} per 9.6 km s^{-1} channel in the center of the field.

3. Results

3.1. The CO velocity field, the globular clusters and planetary nebulae

In Figure 1, we show the ALMA velocity field of CO(J=2-1) where the color wedge units are km s^{-1}. The stars show the position of the GCs (Goudfrooij et al., 2001; Richtler et al., 2014; Sesto et al., 2018) while the dots, the position of the planetary nebulae (McNeil-Moylan et al., 2012). Towards the minor axis of the galaxy (magenta dotted line), a CO velocity gradient is observed from 1600 to 2000 km s^{-1}. The kinematical major axis orientation of the GCs (stars) is quite similar to the photometric minor axis orientation of the galaxy. Accordingly, the CO velocity gradient might be in agreement with the velocity distribution of the GCs and, thus, with the rotation almost perpendicular to the kinematical major axis of the stellar component (orange line) proposed by Sesto et al. (2018). However, a velocity gradient is also present on the CO shell structure (see Fig. 2). This suggests that the complex velocity field observed might not be only explained by a "polar" rotating disk, in agreement with the statement of Morokuma-Matsui et al. (2019). The planetary nebulae show the rotation of the stellar component of the galaxy.

3.2. CO Distribution and Kinematics

In order to study the CO(J=2-1) distribution and kinematics in the inner region of NGC 1316, we derived the moment maps. To obtain those maps, we blanked the pixels with a CO surface brightness below 0.7 Jy beam^{-1} km s^{-1}, which corresponds to 3 times the r.m.s. The CO is detected in different structures such as a shell, clouds, an extended component and a blob (see Fig. 2). At the center of NGC 1316, the measured CO systemic velocity is $\approx$ 1720 km s^{-1}, in very good agreement with the [OII] emission line velocity (1732 ± 10 km s^{-1}) derived by Morokuma-Matsui et al. (2019).

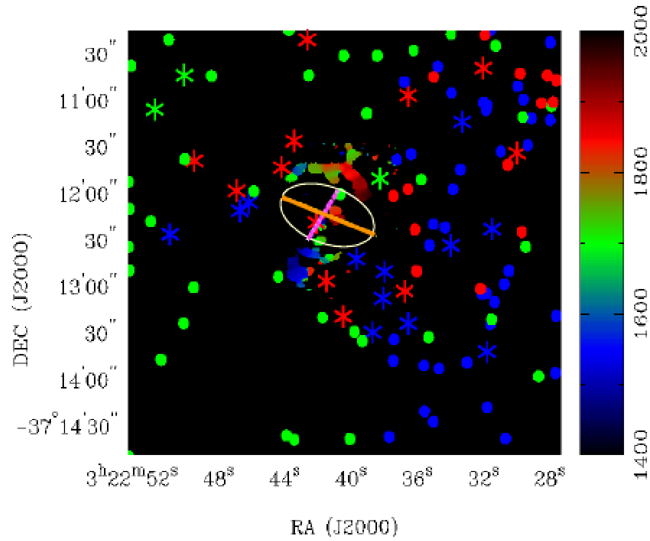

Figure 1: The CO ALMA velocity field of the inner region of NGC 1316, also showing the location of the globular clusters (GCs; stars) and planetary nebulae (PN; dots). The minor axis of the galaxy is marked with magenta dotted line, while the major axis with orange line. The color wedge used for the CO velocity field is also used to indicate the radial velocities reported for the GCs and PNs in the literature.

Table 1: CO(2-1) ALMA flux density for each component

Name	Center [hms dms]	Flux [Jy beam^{-1} km s^{-1}]
Shell	03:22:37.65 −37:11:56.1	77.0 ± 5.0
C1/C2	03:22:40.75 −37:12:15.9	4.7 ± 1.7
C3/C4	03:22:41.81 −37:12:18.2	0.3 ± 0.2
center	03:22:41.81 −37:12:30.1	1.4 ± 1.0
Extended	03:22:42.21 −37:12:38.9	0.8 ± 0.5
Blob	03:22:43.20 −37:15:50.6	40.0 ± 9.0

The high-angular resolution of the ALMA data allow us to trace the dust substructures with greater detail than those shown by Morokuma-Matsui et al. (2019); for example, two compact regions are detected within the shell structure (see Fig. 2). However, we can only measure with a good precision the fluxes of the shell and blob structures (see Table 1). Improvements in the ALMA data reduction processes might result in a better sensitivity, and thus, allow us to get a more precise flux values of the dust clouds.

4. Future work

There are public data from different instruments at various spectral ranges, such as Chandra and HST. In particular, NGC 1316 was observed by Chandra, X-ray Broad (B) band emission ($0.5 - 7.0$ keV; effective energy 2.3 keV). In the near future, we expect to compare the information acquired from the public data available, with that derived from images in narrow-band filters

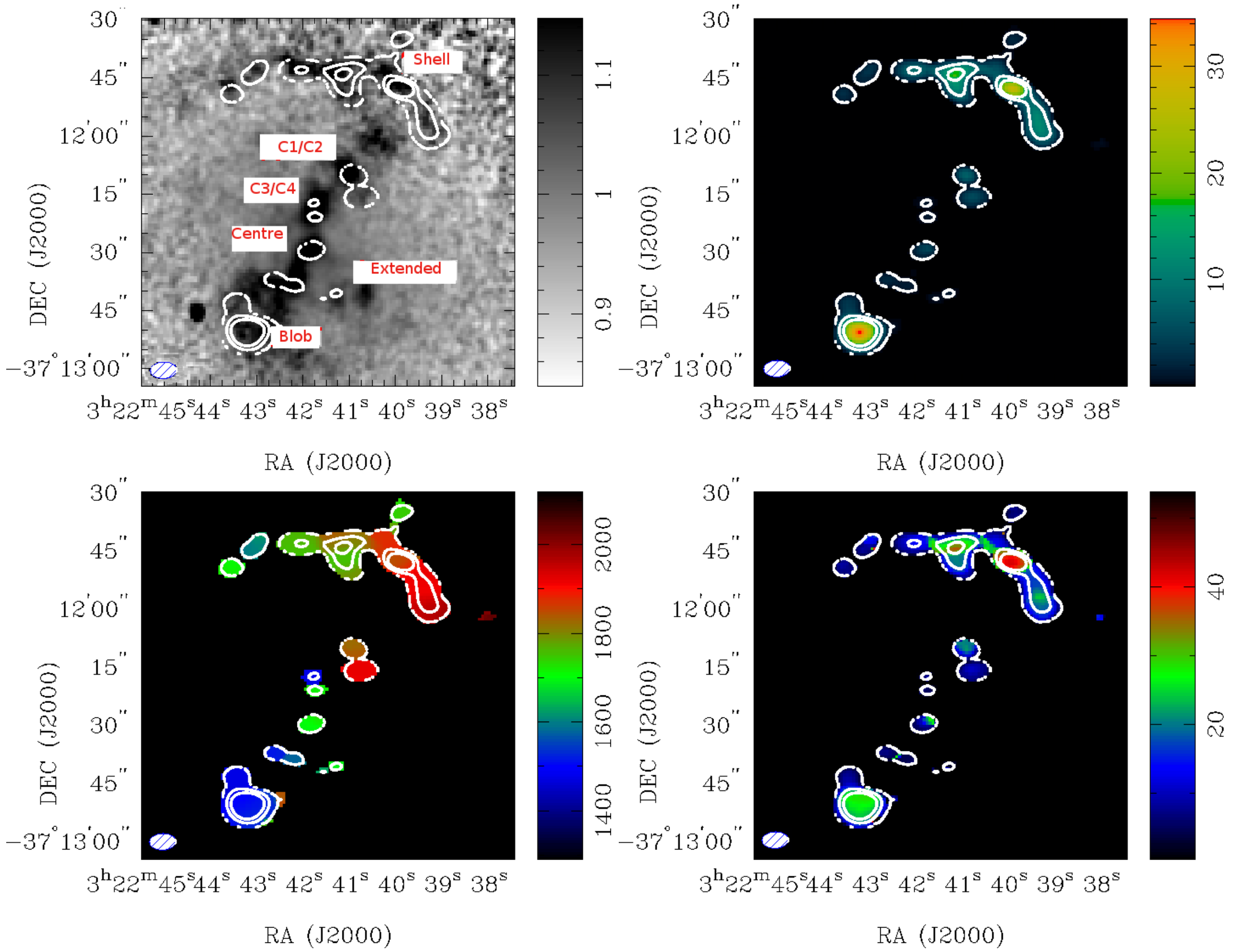

Figure 2: Moment maps of CO(J=2-1) ALMA data cube, corresponding to the inner part of NGC 1316. *Top-left panel:* zeroth moment, CO intensity distribution overlaid to g-i S-PLUS image (Mendes de Oliveira et al. 2019; Smith Castelli et al., this volume). *Top-right panel:* CO intensity distribution map. In white lines, the moment 0 contour levels of $[1, 11, 20]\,3\sigma$, where $\sigma = 0.7$ Jy beam^{-1} km s^{-1}. *Bottom-left panel*: first moment (velocity field, colour bar units km s^{-1}). *Bottom-right panel:* second moment (velocity dispersion, colour bar units km s^{-1}). The synthesized beam is shown in the bottom left corner of each panel.

obtained in the framework of S-PLUS (see Mendes de Oliveira et al. 2019, and Smith Castelli et al. in this volume).

Acknowledgements: JS thanks to FRINGE team members for their useful comments on ALMA data analysis.

References

Cantiello M., et al., 2013, A&A, 552, A106
Duah Asabere B., et al., 2016, A&A, 592, A20
Ekers R.D., et al., 1983, A&A, 127, 361
Goudfrooij P., et al., 2001, MNRAS, 322, 643
Iodice E., et al., 2017, ApJ, 839, 21
Maccagni F.M., et al., 2020, A&A, 634, A9
Mackie G., Fabbiano G., 1998, AJ, 115, 514
McNeil-Moylan E.K., et al., 2012, A&A, 539, A11
Mendes de Oliveira C., et al., 2019, MNRAS, 489, 241
Morokuma-Matsui K., et al., 2019, PASJ, 71, 85
Richtler T., et al., 2014, A&A, 569, A41
Schweizer F., 1980, ApJ, 237, 303
Schweizer F., 1981, ApJ, 246, 722
Sesto L.A., Faifer F.R., Forte J.C., 2016, MNRAS, 461, 4260
Sesto L.A., et al., 2018, MNRAS, 479, 478